Physiologically Based Pharmacokinetic Model for the Inhibition of Acetylcholinesterase by Organophosphate Esters

Jeffery M. Gearhart,[1] Gary W. Jepson,[2] Harvey J. Clewell,[3] Melvin E. Andersen,[4] and Rory B. Conolly[5]

[1]ManTech Environmental Technology, Inc., Research Triangle Park, North Carolina; [2]U.S. Air Force, Wright Patterson, Ohio; [3]Clement International Corporation, Technology, Inc., Ruston, Louisiana; [4]Duke University, Durham, North Carolina; [5]Chemical Industry Institute of Toxicology, Research Triangle Park, North Carolina

Organophosphate (OP) exposure can be lethal at high doses while lower doses may impair performance of critical tasks. The ability to predict such effects for realistic exposure scenarios would greatly improve OP risk assessment. To this end, a physiologically based model for diisopropylfluorophosphate (DFP) pharmacokinetics and acetylcholinesterase (AChE) inhibition was developed. DFP tissue/blood partition coefficients, rates of DFP hydrolysis by esterases, and DFP-esterase bimolecular inhibition rate constants were determined in rat tissue homogenates. Other model parameters were scaled for rats and mice using standard allometric relationships. These DFP-specific parameter values were used with the model to simulate pharmacokinetic data from mice and rats. Literature data were used for model validation. DFP concentrations in mouse plasma and brain, as well as AChE inhibition and AChE resynthesis data, were successfully simulated for a single iv injection. Effects of repeated, subcutaneous DFP dosing on AChE activity in rat plasma and brain were also well simulated except for an apparent decrease in basal AChE activity in the brain which persisted 35 days after the last dose. The psychologically based pharmacokinetic (PBPK) model parameter values specific for DFP in humans, for example, tissue/blood partition coefficients, enzymatic and nonenzymatic DFP hydrolysis rates, and bimolecular inhibition rate constants for target enzymes were scaled from rodent data or obtained from the literature. Good agreement was obtained between model predictions and human exposure data on the inhibition of red blood cell AChE and plasma butyrylcholinesterase after an intramuscular injection of 33 μg/kg DFP and at 24 hr after acute doses of DFP (10–54 μg/kg), as well as for repeated DFP exposures. The PBPK model for DFP was also adapted for the purpose of modeling parathion, including its metabolism to the toxic daughter product paraoxon. The development and validation of this PBPK model for two OPs provides a basis for studying the kinetics and *in vivo* metabolism of other bioactivated organophosphate pesticides and their pharmacodynamic effect in humans. — Environ Health Perspect 102(Suppl 11):51–60 (1994)

Key words: PBPK model, acetylcholinesterase inhibition, organophosphates, diisopropylfluorophosphate, parathion–paraoxon

Introduction

A variety of organophosphate (OP) esters inhibit acetylcholinesterase (AChE) in both central and peripheral nervous tissues resulting in excessive buildup of acetylcholine at neural receptors (*1*). AChE accumulation causes a spectrum of acute toxic effects mediated by the nicotinic, muscarinic, and central nervous system interactions of acetylcholine. These range, depending on dose, from subclinical performance decrements to convulsions, asphyxia, and death (*2*). A model capable of predicting the relationship between OP exposure and resultant toxic effects would be useful in risk assessment and the design of measures protective against exposure to cholinesterase inhibitors. Ideally, the model should be amenable to cross-species scaling and accurately predictive outside the dose range over which its primary validation studies were conducted. Physiologically based pharmacokinetic (PBPK) models meet these criteria (*3–7*). They consist of descriptions of the physiology of the exposed organism and the biochemical processes, which are quantitatively important determinants of toxicant disposition. This includes parameters describing tissue solubilities, metabolism, and binding of the toxicant. A number of PBPK models have been developed for solvents and relatively stable halogenated compounds (*5,8,9*). Additionally, an *in vitro* kinetic model for diisopropylfluorophosphate (DFP) in rat brain has been developed (*10*), and a PBPK model for single dose pharmacodynamics of soman in rats was recently published (*11*).

The goal of this study was to develop a quantitative, physiologically based model of OP pharmacokinetics and AChE inhibition. While AChE inhibition is not a toxic effect per se, it is an index of the probability that acute OP toxicity will occur (*12*). DFP is not itself commercially important, but was chosen for this study as its mechanism of action is thought to be representative of other highly toxic OPs (*12*). Parathion (PA) is an organophosphate insecticide that owes its toxicity to the oxidized product of parathion, paraoxon (PO). The metabolism of PA takes place predominantly in the liver,

This article was presented at the workshop on Pharmacokinetics: Defining the Dose for Risk Assessment held 4–5 March 1992 at the National Academy of Sciences in Washington, DC. Portions of this paper have previously been published as: Gearhart JM, Jepson GW, Clewell III HJ, Andersen ME, Conolly RB. Toxicol Appl Pharmacol 106:295-310 (1990).

This research was conducted under U.S. Department of Defense contract F33615-85-C-0532. Reprints of this article are identified by the Armstrong Aerospace Medical Research Laboratory, Wright-Patterson Air Force Base, Ohio as AL/OE-TR-1994-0123.

The animals used in this study were handled in accordance with the principles stated in the Guide for the Care and Use of Laboratory Animals prepared by the Committee on Care and Use of Laboratory Animals of the Institute of Laboratory Animal Resources, National Research Council, Department of Health and Human Services, National Institute of Health Publication #86-23, 1985, and the Animal Welfare Act of 1966, as amended.

Address correspondence to Dr. J.M. Gearhart, ICF Kaiser, 1201 Gaines St., Ruston, LA 71270. Telephone (318) 255-4800. Fax (318) 255-4960.

but it is also thought that some metabolism of parathion occurs in extrahepatic tissues. The basic model structure described herein for DFP and parathion should be applicable to other OPs whose acute toxicity is mediated by inhibition of AChE.

Development of the Physiologically Based Pharmacokinetic Model

Elements of Model Structure (Overview)

The major determinants of DFP disposition *in vivo* are its hydrolysis by esterases, binding to esterases, tissue solubility, and volatility (leading to exhalation). DFP is metabolized (hydrolyzed) by *A* esterases (AEST) to a noninhibitory product, diisopropylphosphoric acid (DIP). This organophosphate ester also binds to B esterases (BEST) and inhibits their enzymatic activity. The hydrolysis reaction is governed by Michaelis-Menten kinetics whose V_{max} and K_m were determined with *in vitro* assays (Appendix 1). Those compartments described in the model as having A esterase activity (DFPase) are shown in Figure 1 as shaded areas. The binding to and inhibition of B esterases were modeled as bimolecular reactions and were also determined from *in vitro* studies (Tables 1 and 2). All tissue compartments in the model except fat were described as having B esterase activity (*13*). The major determinants of parathion and paraoxon disposition in the model are metabolism of parathion to paraoxon, hydrolysis of paraoxon by esterases, binding of paraoxon to esterases, and the tissue solubility of the parent and daughter compound.

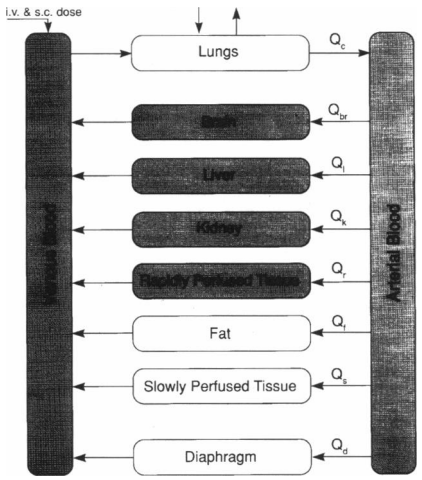

Figure 1. Diagram of the physiologically based pharmacokinetic model for diisopropylfluorophosphate (DFP). The shaded tissue compartments indicate organs within the model in which DFP-ase activity is described. Arrows in and out of the lung compartment indicate inhalation and exhalation of DFP.

Hydrolysis of Diisopropylfluorophosphate

DFP is rapidly hydrolyzed by A esterases (*14*). These enzymes are present in virtually all tissues but often have high activity in the blood. As a result, blood AEST strongly affects the amount of DFP reaching AChE in target tissues. The activity of AEST was obtained from laboratory studies in the rat as described below. The Michaelis–Menten constants K_m and V_{max} were determined for AEST activity in rat brain, blood, liver, and kidney. The K_m for AEST in each of these tissues was assumed to be the same for each of the corresponding mouse tissues. V_{max} values for each of the corresponding mouse tissues were scaled to the 0.7 power of body weight (*8*). DFP also undergoes spontaneous hydrolysis in aqueous solutions. A pseudofirst-order rate of spontaneous hydrolysis was estimated in heat treated (30 min at 60°C) homogenates of each tissue (*10*) and was found to be insignificant (0.0046 min^{-1} relative to the enzymatic rates of DFP hydrolysis (*15*).

Hydrolysis of Paraoxon

The hydrolysis of paraoxon by A esterases was described with Michaelis–Menten kinetics, using data from Wallace and Dargan (*16*), Chemnitius et al. (*17*), and Pla and Johnson (*18*).

Diisopropylfluorophosphate Binding to Esterases

The schema for model simulations of free B esterase, in this case AChE, is shown in Figure 2. The amount of free AChE is determined by the concentration of DFP and 4 different rate constants. The basal level of AChE results from a balance between basal degradation of AChE and synthesis of new enzyme. After exposure to DFP, the amount of free AChE is governed by the balance between the bimolecular rate of inhibition and the rate at which inhibited AChE is regenerated. Once

Table 1. Metabolic constants for pharmacokinetic model of diisopropylfluorophosphate.

	Mouse		Rat		Human	
Organ	V_{max}, mg/hr	K_m, mg/l	V_{max}, mg/hr	K_m, mg/l	V_{max}, mg/hr	K_m, mg/l
Brain	2.28	439.80	9.18	439.80	668	440
Liver	256.58	237.36	1380.00	237.36	52474	237
Kidney	25.61	134.3	103.32	134.3	5042	134
Richly perfused	2.72	50.89	11.04	50.89	560	51
Venous blood	79.38	198.70	320.18	198.7	616	199
Arterial blood	26.46	198.70	106.73	198.7	216	199
Bimolecular rate constants, μM^{-1} hr^{-1}						
Acetylcholinesterase						
	14.16					
Butyrylcholinesterase						
Fast	354.00					
Slow	30.00					
Carboxylesterase						
Fast	1.10					
Slow	0.52					

Table 2. Metabolic constants for a pharmacokinetic model of parathion.

	Parathion desulfuration		Parathion dearylation		Paraoxon hydrolysis	
Organ	V_{max}, mg/hr	K_m, mg/l	V_{max}, mg/hr	K_m, mg/l	V_{max}, mg/hr	K_m, mg/l
Brain	—	—	—	—	9.2	440
Liver	16.6	3.0	28.4	81.8	11	50
Kidney	—	—	—	—	103	134
Richly perfused	—	—	—	—	11	50
Venous blood	—	—	—	—	150	170
Arterial blood	—	—	—	—	100	170

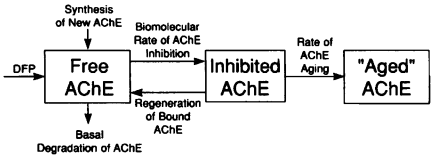

Figure 2. Model for acetylcholinesterase (AChE) inhibition, aging, regeneration, synthesis, and degradation.

AChE is inhibited, it will either return to free AChE, or age and form a permanently inhibited enzyme.

B esterases (*19*) have a serine residue at the catalytic site to which OPs bind, inactivating the enzyme. BESTs include AChE, butyrlcholinesterase (BChE), and carboxylesterase (CaE). While AChE is the target in acute OP intoxication, DFP binding to BChE and CaE is without adverse physiological effect (*20*). Phosphorylated BESTs undergo spontaneous hydrolysis, leading to regeneration of the active enzyme (Figure 2). For DFP, however, this process is relatively slow (*21*) (Table 3). Phosphorylated BEST may also undergo aging (*22*), resulting in a permanent loss of activity (Figure 2). BEST activities were obtained from Maxwell et al.(*13*).

Basal activities of AChE, BChE, and CaE were defined by zero-order synthesis rates (moles binding sites/hour) and first-order loss rates (hr^{-1}; Table 3). First-order loss of rat brain AChE was obtained from Wenthold (*23*), who used radiolabled precursors of AChE to determine enzyme degradation. Synthesis of rat plasma and brain AChE was determined from model optimization of the data of Michalek (*24*), Traina and Serpietri (*25*). The zero-order synthesis rates and first-order loss rates for BESTs in rat plasma and in mice were estimated by fitting simulations to data describing the rate of return of enzyme activity to normal levels over time after DFP dosing (see "Results"). The synthesis and loss rates used for AChE were also used for BChE and CaE since the rate of increase of these activities after OP inhibition is close to that of AChE (*25,26*).

Table 3. Model parameters for AChE inhibition.

	Mouse	Rat	Human
Enzyme inhibition, $\mu M^{-1}\ hr^{-1}$	14.16	14.16[a]	14.16
Enzyme regeneration, hr^{-1}	0.016	0.016[b]	0.016
Enzyme aging, hr^{-1}	0.297[c]	0.263[c]	0.150
Enzyme synthesis, nmole/hr			
Plasma	0.0003[d]	0.0019[e]	0.053
Brain	0.0025[d]	0.0014[f]	0.0014
Enzyme degradation, hr^{-1}			
Plasma	0.060[d]	0.100[e]	0.200
Brain	0.070[d]	0.010[g]	0.010

[a]Data from Jepson (*10*). [b]Data from Vandekar and Heath (*21*). [c]Data from Andersen et al. (*40*). [d]Data from Martin (*34*). [e]Data from Traina and Serpietri (*25*). [f]Data from Michalek et al. (*24*). [g]Data from Wenthold et al. (*23*). The model tracked the inhibition of B esterases in brain, plasma, lung, diaphragm, kidney, liver, and slow and fast compartments. Data and model simulations are shown only for brain and plasma.

Paraoxon Binding to Esterases

The activity of esterases which are inhibited by paraoxon were obtained from Maxwell (*13*).

Metabolism of Parathion to Paraoxon

The metabolism of parathion to its toxic daughter product paraoxon was described in the model to occur in the liver and the kidney by Michaelis–Menten kinetics. The initial K_m and V_{max} for this metabolism were obtained from the work of Wallace and Dargan (*16*). These rates of metabolism were optimized to provide better predictions of parathion and paraoxon pharmacokinetics.

Specification of Compartments

The PBPK model for DFP consisted of both organ-specific and lumped compartments (Figure 1; Appendix 2; Table 4). Organ-specific compartments were used to describe those tissues directly involved in acute DFP toxicity (e.g., brain, lung, diaphragm) or those expected to significantly influence DFP pharmacokinetics (e.g., blood, fat). Blood, though not a target organ, is an important site of DFP metabolism, and blood AChE is a useful reflection of AChE activity in less accessible organs. Separate venous and arterial compartments were used because it has been shown experimentally that there can be significant arterial–venous differences in DFP concentrations (*27*). The kidney and liver are also sites of enzymatic hydrolysis of DFP for which tissue-specific metabolic parameters were readily obtainable. Lumped compartments (fat, rapidly perfused, etc.) were used to describe remaining tissues. The rapidly perfused lumped compartment represented viscera not explicitly described elsewhere. The slowly perfused compartment denoted mainly muscle tissue distributed throughout the organism. Use of lumped compartments helped to preserve a balance between parsimony of model structure, to maintain chemical mass balance, and to describe explicitly mammalian physiology and biochemistry that determine the pharmacokinetic behavior of OPs.

Table 4. Physiological parameters for a pharmacodynamic model of organophosphates.

Parameter	Mouse	Rat	Human
Body weight, kg	0.03	0.22	60.6
Alveolar ventilation, 1/hr	1.04	4.57	354
Cardiac output, 1/hr	1.04	4.57	302
Organ volumes, percentage of body weight			
Brain	1.47	1.16	2.14
Liver	6.17	4.00	4.00
Kidney	1.73	0.73	0.43
Richly perfused	2.00	2.00	3.43
Fat	8.00	7.00	17.00
Slowly perfused	65.74	68.66	55.14
Diaphragm	0.30	0.030	0.3
Lung	0.59	1.15	0.86
Venous blood	5.00	4.00	5.70
Arterial blood	2.50	2.00	2.00
Organ blood flows, percentage of cardiac output			
Brain	3.00	3.00	13.40
Liver	25.00	25.00	27.00
Kidney	20.00	20.00	22.30
Richly perfused	28.00	27.96	20.00
Fat	9.00	9.00	3.60
Slowly perfused	14.40	14.40	13.10
Diaphragm	0.60	0.60	0.60

The PBPK model consisting of mass-balance differential equations and associated computer programs that describe the time-dependent pharmacokinetics of DFP and inhibition of AChE were written in Advanced Continuous Simulation Language (ACSL)(Mitchell and Gauthier Associates, Inc., Concord, MA). Simulations were run on a VAX 8530 (Digital Equipment Co., Maynard, MA).

Laboratory Estimation of Parameter Values

Male Fischer-344 rats (200–250 g at time of use) were obtained from Charles River Breeding Laboratories (Wilmington, MA). They were housed in plastic shoe box cages with hardwood chip bedding, two per cage, on a 12-hr light and dark cycle. Food (Purina Formulab #5008) and water were available *ad libitum*. Animals were quarantined for 2 weeks to allow for acclimatization and for quality assurance procedures designed to ascertain animal health.

Quantitation of Diisopropylfluorophosphate Metabolism

Enzymatic Hydrolysis. V_{max} and K_m estimates were obtained by measuring fluoride ion appearance in rat tissue-saline homogenates (1:9 w/v) stirred constantly at 37°C (Table 3). Standards were prepared in distilled water. Fluoride was measured with an Orion 701 digital Ionalyzer equipped with an Orion 96-09 combination fluoride

electrode (*10*). Heat-treated (30 min at 60°C) homogenates of each tissue were used to measure nonenzymatic DFP hydrolysis. V_{max} and K_m were estimated from Lineweaver-Burk plots of the data (*28*). V_{max} values for DFP metabolism determined in rat tissues were scaled for mice and humans by 0.7(body weight) (*8,29*). The rat K_m was used without adjustment for mouse and human simulations.

Bimolecular Inhibition Rate Constants. The rate of reaction of DFP with AChE, BChE, and CaE, corresponding to the rate of esterase inhibition, was obtained by measuring decreases in tissue homogenate esterase activity after addition of DFP (Table 1). AChE activity was assayed with a modification of the method of Ellman (*30*). Assays were initiated by adding 20 µ of tissue-saline homogenate (1:3 w/v) to 2.0 ml of substrate solution (0.3 mM acetylthiocholine [Calbiochem, San Diego, CA], 0.3 mM dithionitrobenzoic acid [Calbiochem, San Diego, CA] in 0.05 M potassium phosphate buffer [Pfaltz and Bauer, Stanford, CT]) that had been previously warmed in a water bath at 37°C. After rapid mixing, 0.3 ml of the homogenate/substrate mixture was immediately added to a temperature-controlled cuvette (*37*) in a Gilford 2600 spectrophotometer (Oberlin, OH). The cuvette was held for 1 min and then absorbence was read at 0.1-min intervals for 1 min. DFP (Sigma Chemical Co., St. Louis, MO) was then added and the absorbence read at 412 nm at 0.1-min intervals for 5 min. The bimolecular inhibition rate constant was evaluated as

$$-k_i = (\ln(V/Vo)/t)(K_m+[S])/K_m \times [\text{DFP}] \quad [1]$$

where k_i is the bimolecular rate constant ($M^{-1}min^{-1}$); $[S]$ is the substrate concentration (M); V is the reaction velocity (mole/min/g tissue), Vo is the AChE activity at time zero (mole/min/g tissue); t is the duration (min) of incubation; [DFP] is the concentration of DFP (M), K_m is the Michaelis–Menten constant (M). The appropriate volume of DFP was added and there was a plot of absorbence at 412 nm versus time obtained. Slopes of tangents to the curve provided the velocity of the substrate hydrolysis reaction. The bimolecular rate constants for BChE and CaE were determined as for AChE, except that the substrates were butyrylthiocholine and *p*-nitrophenylacetate, respectively. The concentration of tissues used in tissue homogenates was not a factor in these calculations as inhibition reaction rates were determined per gram of tissue.

Partition Coefficients

Partition coefficients for DFP (Table 5) were determined by the vial equilibration technique (*31,32*). DFP was injected into a closed vial containing heat-treated (60°C, 1 hr) rat blood or tissue homogenate at 37°C. After equilibration (2 hr), head space DFP space was quantitated by gas chromatography. Reference vials containing saline were treated identically. Tissue–blood partition coefficients were calculated by dividing the tissue–air value by that for blood–air. Partition coefficients determined for rat tissues were also used for simulations of mouse and human data. The muscle–blood partition was used for the lumped, slowly perfused compartment and the liver–blood partition for the lumped richly perfused compartment. The partitioning of parathion in the brain compartment was estimated from the data of Eigenberg et al. Parathion and paraoxon partitions in other tissues were determined *in vitro* by equilibrium dialysis (*33*).

Table 5. Partition coefficients.

Tissue	Partition coefficients		
	DFP	Parathion	Paraoxon
Blood–air	12.57	NA	NA
Brain–blood	0.67	4.56[a]	2.31[a]
Liver–blood	1.53	5.21	6.62
Kidney–blood	1.63	5.21	6.62
Richly perfused blood	0.67	5.21	6.62
Fat–blood	17.6	101.2	10.22
Slowly perfused blood	0.77	2.55	3.62
Diaphragm–blood	0.77	2.55	3.62

DFP, diisopropylfluorophosphate. [a]Estimated from Eigenberg (*37*).

Results

Diisopropylfluorophosphate Pharmacokinetics and Acetylcholinesterase Inhibition in Mice

Several published studies of DFP pharmacokinetics and AChE inhibition in mice and rats were analyzed with the simulation model. This included both single and mul-

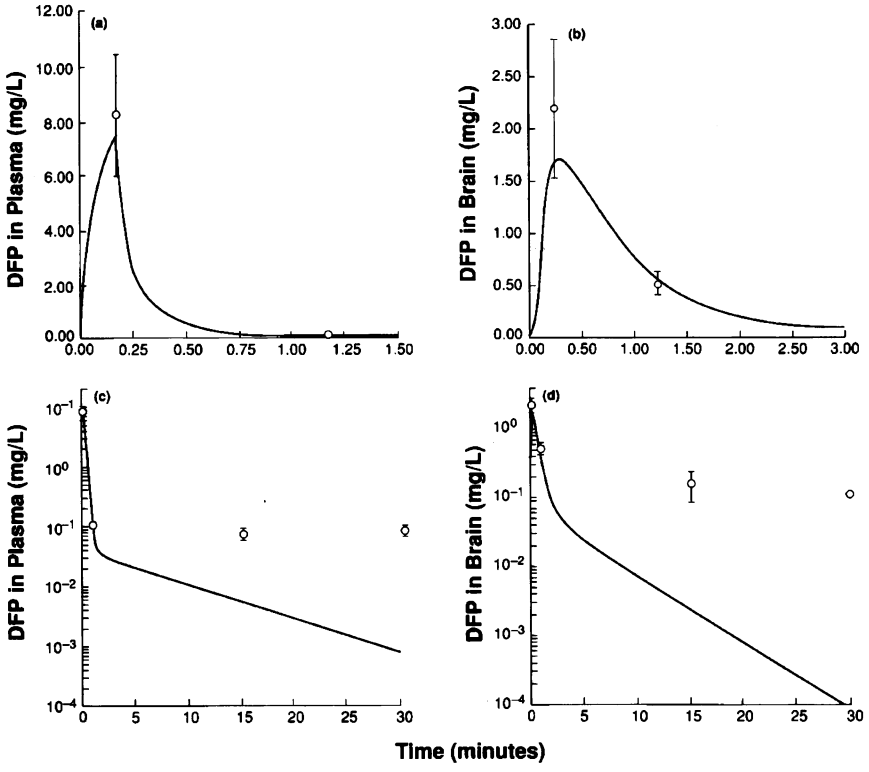

Figure 3. Time-course of free diisopropylfluorophosphate concentration (DFP) (milligrams per liter) in plasma and brain in male mice (Dublin ICR) after tail vein injection of 1 mg DFP/kg. Each datum represents the mean (±1 SD) of five animals. Data from Martin (*34*). Solid line depicts computer simulation generated with the physiologically based pharmacokinetic model.

tiple dosing regimens. Martin (*34*) injected Dublin ICR male mice (Dominion Laboratories, Dublin, VA) via the tail vein with 1 mg tritium [^{3}H]DFP/kg. To measure free, bound, and metabolized [^{3}H]DFP, tissues from treated animals were homogenized, centrifuged, and extracted with ethyl acetate. The ethyl acetate extracts were then either counted with liquid scintillation for total radioactivity, concentrated under nitrogen (N_2), and subjected to thin-layer chromatography, or the aqueous portion that remained after extraction was solubilized and counted for radioactivity.

A dominant characteristic of DFP pharmacokinetics well illustrated by this study is rapid clearance of free DFP from blood and brain. Free DFP in plasma had largely disappeared within 1 min of iv injection (Figure 3*a*). In brain, free DFP at approximately 1 min post injection had fallen to a small fraction of its peak concentration (Figure 3*b*). The PBPK model accurately simulated these data (Figure 3*a,b*). At time points greater than 5 min though, a less rapid disappearance of DFP from blood and brain than was predicted by the model was measured experimentally (Figure 3*c,d*). However, the area under the plasma and brain concentration–time curves at these later time points represented less than 3% of the total free DFP dose to these tissues. It is possible that the apparent failure of the model to accurately track the free DFP concentration at later time points may be due to the measurement of ^{3}H activity as a surrogate for the actual concentration of free DFP. Some ^{3}H activity inferred to be free DFP may, in fact, have been a DFP metabolite or products of covalent binding.

Martin (*34*) also measured AChE inhibition in mice after iv injection of DFP. The nadir of AChE activity occurred within 1 min in plasma and at about 5 min in brain (Figures 4*a*,5*a*). After optimization of AChE resynthesis, PBPK model simulations of these data were reasonably accurate from the time of injection through 24 hr (Figures 4*b*,5*b*). The PBPK model was initially structured so that plasma and brain tissue AChE activities would return to 100% of control levels in about 3.75 days. Martin (*34*) found, however, that 7 days after a single iv injection of 1 mg DFP/kg, brain AChE activity in the mouse was only about 80% of the preexposure level (Figure 5*c*).

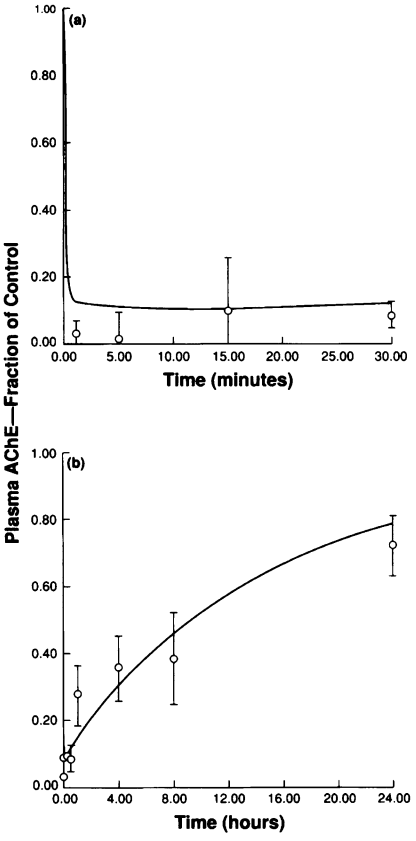

Figure 4. Time-course of plasma acetylcholinesterase (AChE) activity in male mice (Dublin ICR) after tail vein injection of 1 mg diisopropylfluorophosphate/kg. Data are expressed as a fraction of control activity. Each datum represents the mean (±1 SD) of five animals. Data from Martin (*34*). Solid line depicts computer simulation.

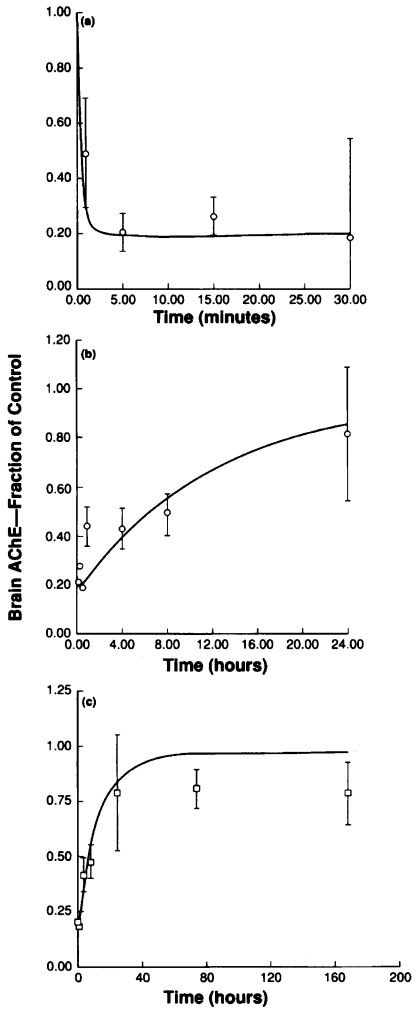

Figure 5. Time-course of brain acetylcholinesterase (AChE) activity in male mice (Dublin ICR) after tail vein injection of 1 mg diisopropylfluorophosphate/kg, expressed as a fraction of control (AChE) activity. Each datum represents the mean (±1 SD) of five animals. Data from Martin (*34*). Solid line depicts computer simulation.

Acetylcholinesterase Inhibition in Rat Plasma and Brain after Repeated Dosing with Diisopropylfluorophosphate

Michalek (*24*) injected male Wistar rats sc with DFP every second day for 22 days. The first dose was 1.1 mg DFP/kg, and subsequent doses were 0.7 mg/kg. Five rats (four DFP and one vehicle exposed) were sacrificed for measurement of brain AChE activity at 1.5 and 24 hr after the 1st, 2nd, 4th, 6th, 9th, and 12th DFP doses and at various intervals (48 and 72 hr; days 7, 14, 28, and 35) after the last dose. Traina and Serpietri (*25*) measured the effect of DFP on plasma AChE activity using the same rat strain and dosing regimen as Michalek (*24*).

Traina and Serpietri (*25*) found that plasma AChE activity in the rat fell rapidly after sc injection of DFP (Figure 6*a*). AChE activity was about 15% of control 1.5 hr after the initial dosing and about 70% of control at 24 hr. Simulations of these data (Figure 6*a*) were obtained after optimization of the rate of absorption of DFP into blood following a single sc injection. Simulation of the initial fall in plasma AChE activity was particularly sensitive to this parameter. The rate of AChE synthesis and first-order loss were also visually optimized against these data. This was critical to successful simulation of the return of AChE activity towards control levels obtained after a single sc injection. Once obtained in this manner the model was used for simulation of the multiple dosing scenario (Figure 6*b*).

Plasma AChE activities measured (*25*) after the last subcutaneous dose of DFP (day 22) are suggestive of an overshoot of the control level. Plasma AChE activity

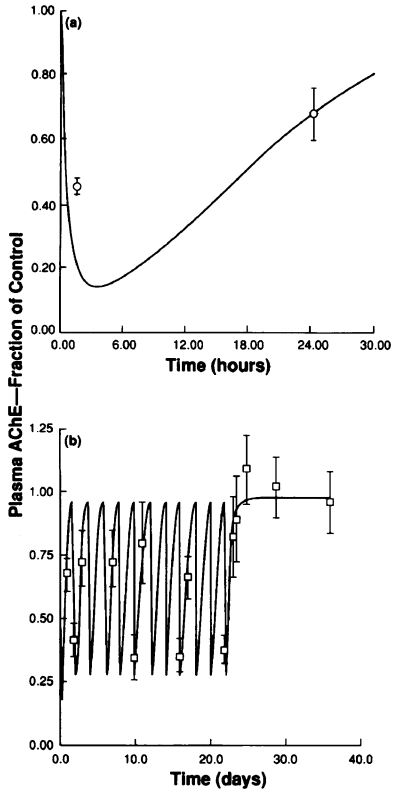

Figure 6. Plasma acetylcholinesterase (AChE) activity in male rats (Wistar) injected sc with diisopropyl fluorophosphate (DFP) (a first dose of 1.1 mg DFP/kg, then 0.7 mg/kg every other day for 22 days). Data are expressed as a fraction of the control AChE activity. Plasma AChE activity was assayed at 1.5 and 24 hr after each dose of DFP. Each datum represents the mean (±1 SD) of four animals. Data from Traina and Serpietri (*25*). Solid line depicts computer simulation.

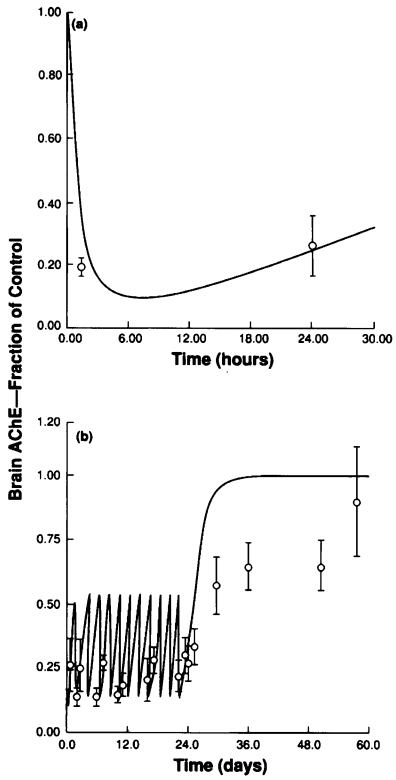

Figure 7. Brain acetylcholinesterase (AChE) in male rats (Wistar) injected sc with diisopropylfluorophosphate (DFP) (a first dose of 1.1 mg DFP/kg, then 0.7 mg/kg every other day for 22 days). Data are expressed as a fraction of control AChE activity. Brain AChE activity was assayed at 1.5 and 24 hr after DFP dosing. Each datum represents the mean (±1 SD) of six animals. Data from Michalek et al. (*24*). Solid line depicts computer simulation.

had returned to a stable 100% of the control level by 5 to 6 days after the last DFP dose (Figure 6*b*). There was no provision in the PBPK model for simulation of such an overshoot, though this phenomenon has been modeled for other systems, as in the case of glutathione replacement after depletion by toxicant exposure (*35,36*).

The pattern of brain AChE activity after subcutaneous DFP dosing (*24*) was similar to that seen in plasma (*25*), though the extent of recovery between doses was smaller (Figure 7*a,b*). The recovery of brain AChE activity after termination of DFP dosing was prolonged. For example, activity was only about 65% of control 28 days after the last dose of DFP. When the basal rates of AChE degradation and synthesis were optimized for acceptable simulation of brain AChE activity during dosing (Figure 7*a*), simulation of AChE activity after termination of dosing predicted a more rapid return than was observed (Figure 7*b*). Model structure dictated a relatively rapid and monophasic return of brain AChE activity to the original control level. The data suggest, however, that a full return of brain AchE activity to the control level is a multiphasic process.

Acetylcholinesterase Inhibition in Humans

Simulations of both the acute and repeated DFP exposures provide predictions of AChE and BChE inhibition that are very near the experimentally determined human values. The time-course of AChE and BChE inhibition after an acute dose of 33 µg DFP/kg bw resulted in a maximum AChE inhibition at 24 hr and maximum BChE inhibition at 4 hr (Figure 8*a*). This difference in the degree and time to maximum enzyme inhibition is a direct reflection of the 20-fold difference in the bimolecular inhibition rate constants for the two enzymes. The simulation provided a good prediction of AChE inhibition for all the acute time-course inhibition data. Simulations of red blood cell (RBC)–AChE and plasma BChE inhibition in four people injected at four different doses of DFP covering 10 to 54 µg DFP/kg bw compared favorably to the actual enzyme activity measured in these individuals at 24 hr (Figure 8*b*). The greatest discrepancy between the simulations and data occurred for the RBC–AChE at 54 µg/kg dose and the 10 µg/kg plasma BChE values (Figure 8*b*).

The model predictions of AChE and BChE inhibition resulting from repeated im injections of 20 µg DFP/kg bw were representative of the overall trend of enzyme inhibition (Figure 8*c*). During the first 5 days of repeated dosing, the actual AChE activity dropped rapidly from 100% of baseline to approximately 50% activity and then at a much slower rate to a final enzyme activity of 30%. The simulation of these data predicted a inhibition of approximately 40% during the initial 5 days of dosing that was sustained throughout the rest of the exposure period. BChE activity dropped immediately during the first 5 days to 15% of the basal enzyme activity and remained at this level during the exposure period (Figure 8*c*). The simulation predicted a 10 to 20% greater initial drop in enzyme activity then was actually measured.

Parathion and Paraoxon Kinetics in the Rat

Eigenberg (*37*) measured concentrations of PA and PO in brain, liver, and blood, as well as PA in fat, following an iv injection of PA at a dose of 3 mg/kg. Simulation of PA and PO kinetics in brain, liver, and blood after iv injection of 3.0 mg PA/kg were in general agreement with the published data (Figures 9,10). The simulation of PA kinetics in fat tissue (Figure 11) required the addition of diffusion limitation to this compartment to achieve agreement with the experimental data.

Discussion

The Michaelis–Menten parameters used to describe DFP hydrolysis and the bimolecular inhibition rate constants describing BEST inhibition were obtained *in vitro*. The success of simulations of *in vivo* DFP pharmacokinetics data (Figure 3*a,b*) suggests that the parameter values measured *in vitro* are reasonable estimates of the corresponding *in vivo* values. *In vitro* estimation of *in vivo* parameter values was also used by Dedrick (*3*). They developed a PBPK model for arabinofuranosylcytosine (ARA-C) and

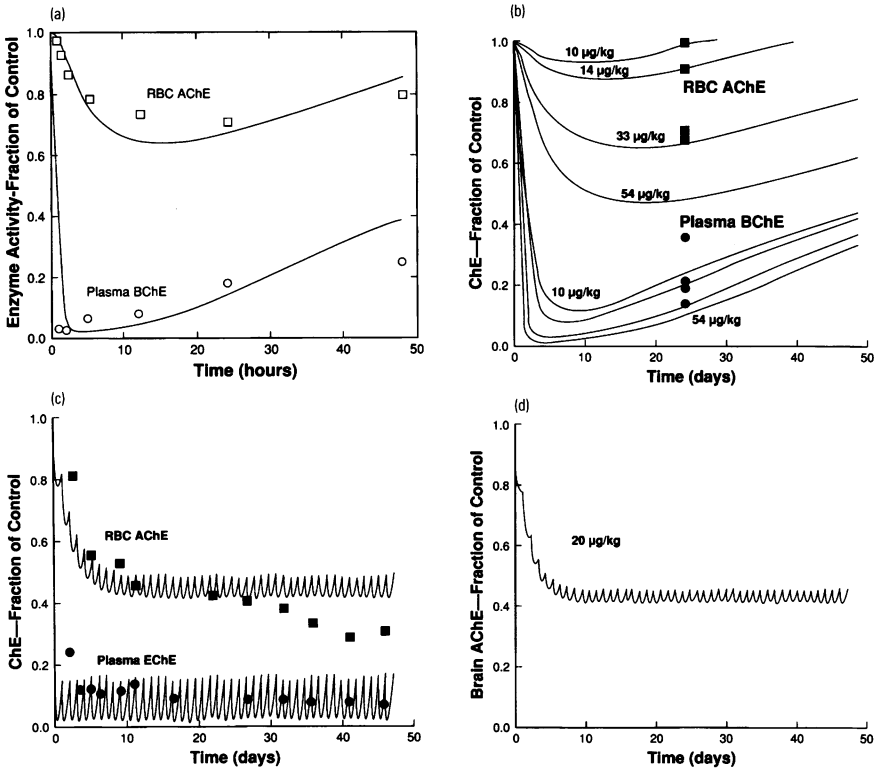

Figure 8. (*a*) Time-course of red blood cell acetylcholinesterase (AChE) and plasma butyrlcholinesterase (BChE) activities in a human after an im injection with 33 µg diisopropylfluorophosphate (DFP)/kg. (*b*) Twenty-four hour values for red blood cell AChE and plasma BChE activities in four humans after an im injection with from 10 to 54 µg DFP/kg. (*c*) Average values for the time-course of red blood cell AChE and plasma BChE activities in 35 human subjects after daily im injections with an average of 20 µg DFP/kg/day. (d) Predicted inhibition of human brain AChE activity after an acute im dose of 20 µg DFP/kg/day. Data for *a, b,* and *c* are expressed as a fraction of control activity. Solid lines depict computer simulation. Data from Grob et al. (*47*).

its metabolite, arabinofuranosyluracil in four species and used rates of ARA-C metabolism measured *in vitro*. However, Reitz (*38*) found significant *in vitro* and *in vivo* differences in the rates of methylene chloride metabolism. Clearly, this problem must be considered on a case-by-case basis. Good agreement between *in vitro* and *in vivo* metabolic rates might be expected when the enzyme is soluble and its activity is not directly dependent on cofactor concentration (e.g., phosphorylphosphatases) (*17*). In such cases it should be relatively easy to create an *in vitro* milieu functionally similar to the *in vivo* milieu. On the other hand, some enzymes are embedded in cellular membranes, have specific orientations with respect to other enzymes that preprocess substrates, and have activities highly dependent on cofactor concentrations (e.g., cytochrome P450) (*39*). Activities of the latter type may be greatly affected by tissue homogenization and dilution in buffer. The results obtained in this study and in the studies of Dedrick (*3*) and Reitz (*38*) are consistent with this expectation.

The rate of AChE inhibition is a function of the bimolecular rate constant, k_i. The k_i for AChE was determined in rat brain homogenate and this value was then used in all model compartments having this enzyme activity. The rat k_i for AChE was also used for mice. This approach was also used for the DFP-esterase inhibition rate constants for CaE and BChE (see section on model development). The ability of the PBPK model to simulate AChE inhibition in mice and rats (Figures 4–7) indicates that the variance in these rate constants among tissues and species is not large. Andersen (*40*) found the rates of inhibition for solubilized AChE from the cerebral cortex of mice was within 20% of the rate for rats.

One goal of this research effort was to predict the kinetics and AChE inhibition not only after an acute exposure to DFP, but also after repeated doses. A good simulation of the experimental data for plasma and brain AChE inhibition in rats during repeated subcutaneous administration of DFP was achieved (Figures 6,7). The experimentally measured return of brain AChE activity was much slower than the rate of enzyme resynthesis that was used in the model. If the brain AChE resynthesis rate was decreased in the model to agree with the rate of experimentally determined postexposure synthesis, then predictions of brain AChE activity during DFP dosing would be underestimated.

The experimentally determined activity of AChE in brain after each DFP dose was reproducible, yet the levels of AChE at the 48- and 72-hr time points at the end of all repeated dosing indicated there was an alteration in the mechanisms controlling enzyme synthesis. For the model to predict the return of brain AChE to normal levels of activity after repeated dosing, it would be necessary to address the effects of down regulation of AChE receptors on AChE enzyme synthesis rates. The simulation of AChE resynthesis used the preexposed level of AChE activity as a reference in setting the rate of resynthesis. This assumed that the

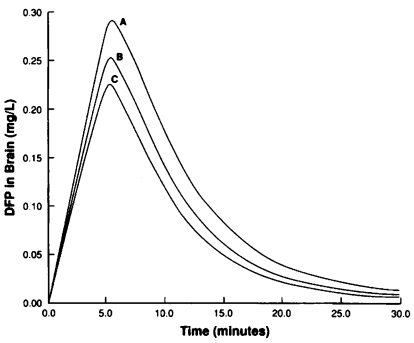

Figure 9. Simulated concentration of diisopropylfluorophosphate in human brain (mg/l) after a 5-min inhalation at 50 ppm. The level of plasma A esterates for curve A was 1.5 times the scaled activity; for curve B it was the scaled level of activity; and for C, it was 50% of the scaled activity.

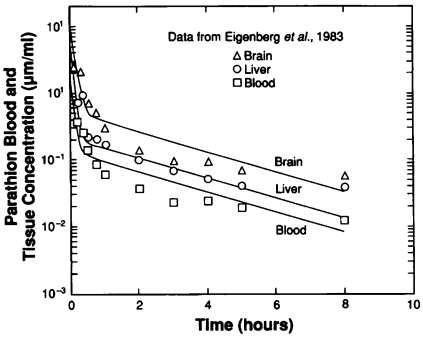

Figure 10. Time-course of parathion in blood, liver, and brain in (µg/ml) for 8 hr after an iv injection of parathion at a dose of 3 mg/kg. Each data point represents the mean of four rats. Data from Eigenberg et al. (*37*).

receptor affinity and impetus to return AChE to control tissue levels was unaltered. If the receptor numbers and affinities are affected by repeated dosing with DFP, it would alter the rates of AChE resynthesis experimentally, which would require a change in the model parameter controlling AChE synthesis. This effect is believed to be a response to excessive tissue concentrations of acetylcholine after AChE inhibition (*41*).

Clarification of the mechanism of this tolerance has involved the measurement of receptor binding and numbers. Binding of quinuclidinyl benzilate, a muscarinic affinity label, has been shown to decrease in affinity and density in the striatum of rats following chronic cholinesterase inhibition with DFP (*42*). Yamada (*43*) was able to demonstrate a correlation between and a dose-dependent decrease in muscarinic receptors, AChE activity, and choline uptake in regions of the brain and gastrointestinal tract of guinea pigs treated repeatedly with DFP. This effect was antagonized by physostigmine and atropine.

Simulations of the 24-hr recovery of brain AChE after repeated DFP dosing were well within one standard deviation of the data during the series of DFP doses and only failed to predict brain AChE levels after dosing had ceased. This could be due to the experimental protocol chosen by Michalek (*24*), where 48 hr were allowed between each successive dose of DFP. Ehlert (*42*) has shown the half-time for the loss of muscarinic binding sites to be approximately 1.6 days. The difference between the frequency of DFP dosing Michalek (*24*) used (i.e., which we have simulated) and the rate of change in receptor numbers and affinity may have been lessened by the repeated dosing until after the completion of dosing.

While there was a good prediction of DFP pharmacokinetics shortly after injection that accounted for greater than 95% of the material injected, the simulation and data became more divergent at longer times after dosing. After the initial injection of DFP, the major model parameter affecting the disappearance of compound from the animal is AEST hydrolysis activity. It would be expected that enzymatic hydrolysis of DFP would continue to decrease blood and tissue concentrations until there is total disappearance of the compound. The experimental data showed no difference in plasma DFP concentrations between 15 and 30 min after injection and only a decrease in DFP concentration of 32% in brain. Those BEST enzymes with the highest affinity for DFP already would have become inhibited at this time and their low molar concentration then would have very little effect on the overall kinetics of DFP. Because the model and data both predict the amount of DFP present in blood and brain to be in the picogram per milligram range within minutes of injection, it is possible that the difference between the data and simulations are due to inexact compound identification involved in using the combination of radiolabel and chemical extraction to quantitate very low concentrations of DFP.

The PBPK model initially developed to describe the kinetics of DFP and inhibition of AChE in the rodent was successfully scaled to simulate data from humans repeatedly treated therapeutically with DFP. It was possible to predict the time course of inhibition of RBC AChE and plasma BChE in a male human injected intramuscularly with a 33 μg/kg dose of DFP and these enzyme activities at 24 hr in four different humans injected with DFP at doses from 10 to 54 μg/kg. By using the data from human studies to validate the model, it is possible to simulate the amount of AChE inhibition in other target organs for which there are no human data (Figure 12). This is significant, because it provides a means of predicting OP effects in the target organs of humans for which there will probably never be data. The development of this model to predict the human response to organophosphate exposure provides a method of modeling possible therapeutic or prophylactic approaches for organophosphate exposure in humans.

The model was exercised for a hypothetical inhalation exposure of humans to 50 ppm DFP for 5 min. Because CaE has been shown to be an important detoxification route for soman (*20*), a simulation of human exposure to DFP was conducted with the activity of CaE decreased by a factor of 10, which is the activity expected in humans (*44*). The effect of this alteration of CaE levels on the kinetics and inhibition of AChE was negligible due to the much lower affinity of CaE for DFP relative to the other enzymes present (Table 1). The parameter that did have an effect on DFP blood and brain kinetics was AEST activity in the blood. The levels of AEST in blood were decreased by one-half and increased by one-half over the amount that was scaled by (body weight)$^{0.7}$ from rats to humans. A 50% decrease in AEST activity in blood caused a 16% increase in the peak concentration of DFP in brain. In contrast, increasing DFP AEST activity by 50% caused an 9.5% decrease of DFP in blood and a 13% decrease in brain.

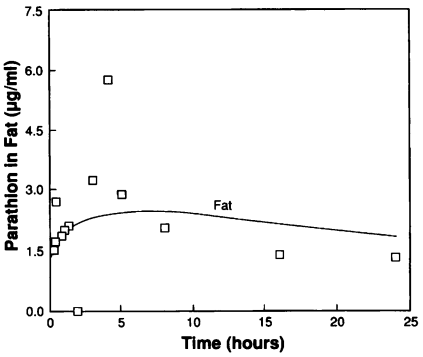

Figure 11. Time-course of parathion in fat (μg/ml) for 24 hr after an iv injection of paraoxon at a dose of 3 mg/kg. Each data point represents the mean of four rats. Data from Eigenberg et al. (*37*).

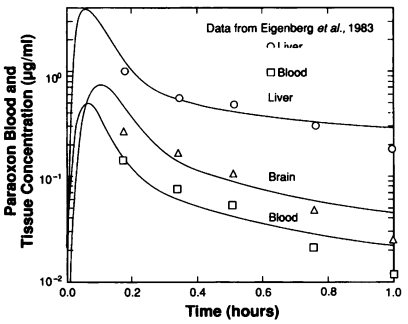

Figure 12. Time-course of paraoxon in liver, brain, and blood in (μg/ml) 1 to 3 hr after an iv injection of parathion at a dose of 3 mg/kg. Each data point represents the mean of four rats. Data from Eigenberg et al. (*37*).

The PBPK model for DFP was successfully modified to describe the time-course of parathion and paraoxon in blood, liver, and brain, and the time-course for parathion in fat. A preliminary validation of the model was conducted with data obtained from the literature and collected in laboratory studies. It was possible to provide a reasonably good simulation of *in vivo* data obtained from the literature, but this required adjustment of enzymatic values obtained in the literature. With further validation of the model, it will be possible to predict the inhibition of AChE in the different tissue compartments of the target organs and use this model to provide predictions of the degree of AChE inhibition in occupational situations where humans may be exposed. This will then provide a basis for using the model to perform risk assessments of different exposure scenarios.

The PBPK model for OPs is in effect a quantitative hypothesis specifying the factors controlling OP pharmacokinetics in

rats, mice, and humans. Once its parameters have been set to realistic values, the ability of the model to simulate real data becomes a test of the hypothesis. Failure to accurately simulate data suggests that model structure, the hypothesis, needs refinement. Iterations of this process (i.e., model refinement, predictive simulation, laboratory experimentation) can be exploited to advance the understanding of the biological determinates of OP biodistribution. This general paradigm has recently been discussed by Clewell and Andersen (*45*).

The present model for OPs does not simulate toxicity per se. Instead, AChE inhibition is simulated as an index of the likelihood of toxic effect (*2*). The acute toxicities of some OP agents may not be due to acetylcholine overload but rather to actions at sites other than AChE (*46*). In these cases, simulation of the concentration of free OP in target tissues would be expected to provide an index correlated with toxicity. For OPs whose primary mechanism of acute toxicity is not AChE inhibition, it would be desirable to extend the current PBPK model to explicitly describe the OP–tissue interaction most directly correlated with toxicity.

PBPK models are useful in risk assessment because their structure is amenable to cross-species scaling or to simulate exposure scenarios that cannot be tested otherwise. A PBPK model validated for experimental animals and appropriately scaled to humans is theoretically capable of simulating pharmacokinetic behavior in humans. This assumes that the model structure appropriate for the experimental species is also appropriate for humans. Physiological parameters such as organ volumes, organ blood flows, and pulmonary ventilation rates are well characterized for humans as well as for common experimental animals. Scaling of toxicant-specific parameters can be more problematical. Some success in scaling of PBPK models has been achieved by assuming that metabolic rates [e.g., V_{max}, scale in proportion to body surface area (*8*)]. With respect to the DFP model, it is not clear *a priori* how the DFP–esterase bimolecular inhibition rate constants should scale from rodents to humans. The ability demonstrated in rats and mice to successfully use *in vitro* estimates of parameter values for simulation of *in vivo* data suggested the same approach would work in the human version of the model. Moreover, the similarity of inhibition rates for solubilized AChE from the cerebral cortex of mice and rats (*40*) implies that some parameter values may be relatively insensitive to large changes in body weight.

In summary, the model structure used in the present study is clearly relevant to humans for a variety of OPs (*2*) and the data required for scaling is explicitly specified by this structure. Application of the present model to other OPs of concern for human exposure may, therefore, be a relatively straightforward task.

Appendix I: Conversion of *In Vitro* Measurements for *In Vivo* Modeling

The two calculations shown here provide an example of the dimensional analysis to convert *in vitro* DFPase values of V_{max} and K_m for extrapolation to *in vivo* modeling. The values in Table 3 for V_{max} are reported in milligrams per hour. These values were determined *in vitro* in grams per minute per gram of tissue. The *in vitro* value for K_m was determined in nanomoles per liter. An example of converting *in vitro* values to *in vivo* values for the liver is, for V_{max}, 9.02 mole DFP/min/g liver × 60 min/hr 40 g liver/kg bw × 0.184 g/μmole × mg/10^3g = 3983 mg/hr × kg and, for K_m, 1.29 mmoles/l × 184 mg/mmole = 237.36 mg/l.

Appendix II: Description of Pharmacokinetic Model

The mass balance differential equation for DFP in brain is $VBr \times dCBr/dt = QBr \times (CABr - CVBr) - (V_{max}Br \times CVBr)/(K_mBr + CVBr) - KAChE \times CAEBr \times CBr - KCaE \times CCEBr \times CBr - KBChE \times CBEBr \times CBr$, where VBr = volume of brain (liter); CBr = concentration of DFP in the brain compartment (mg/l); QBr = blood flow to the brain (l/hr); $CABr$ = DFP in arterial brain (mg/l); $CVBr$ = DFP in venous blood leaving brain (mg/l); $V_{max}Br$ = maximum rate of DFPase hydrolysis (mg/hr); K_mBr = Michaelis-Menten constant for DFPase in brain (mg/l); $KAChE$ = bimolecular rate constant for DFP reaction with AChE $(M\text{-}hr)^{-1}$; $CAEBr$ = AChE concentration in brain (M); $KCaE$ = bimolecular rate constant for DFP reaction with CaE $(M\text{-}hr)^{-1}$; $CCEBr$ = CaE concentration in brain (M); $KBChE$ = bimolecular rate constant for DFP reaction with BChE $(M\text{-}hr)^{-1}$; and $CBEBr$ = BChE concentration in brain (M). This equation is also used to describe DFP in the liver, kidney, rapidly perfused, as well as venous and arterial tissue compartments. In the remaining compartments (lungs, fat, slowly perfused, and diaphragm), the differential equation for DFP is $VT \times dCT/dt = QT \times (CAB - CT/PT)$, where VT = volume of tissue (liter); dCT/dt = change in tissue concentration with time (mg/hr); QT = blood flow to tissue (l/hr); CAB = arterial blood concentration (mg/l); CT = tissue concentration (mg/l); and PT = tissue-to-blood partition coefficient.

The differential equation to calculate inhibited AChE activity in the different tissue compartments is $VBr \times dAEBR/dt = (KAChE \times CAEBR \times CBRM) - (KRABR \times AEBR - (KAABR \times AEBR)$, where VBr = volume of brain (l); $KAChE$ = bimolecular inhibition rate constant of ACHE $(M\text{-}hr)^{-1}$; $CAEBR$ = free AChE in brain (M); $CBRM$ = DFP in brain (M); $KRABR$ = rate of regeneration of inhibited AChE (hr^{-1}); $AEBR$ = inhibited AChE (M); and $KAABR$ = rate of aging of inhibited AChE (hr^{-1}).

REFERENCES

1. Koelle GB. Organophosphate poisoning-an overview. Fundam Appl Toxicol 1:129–134 (1981).
2. Murphy SD. Toxic effects of pesticides. In: Casarett and Doull's Toxicology (Klaassen CD, Amdur MO, Doull JD, eds). New York:Macmillan Publishing, 1986;519–581.
3. Dedrick RL, Forrester DD, Cannon JN, El Dareer SM, Mellett LB. Pharmacokinetics of 1-B-D-Arabinofuranosylcytosine (ARA-C) deamination in several species. Biochem Pharmacol 22:2405–2417 (1973).
4. King FG, Dedrick RL, Collins JM, Matthews HB, Birnbaum LS. Physiological model of the pharmacokinetics of 2,3,7,8-tetra- chlorodibenzofuran in several species. Toxicol Appl Pharmacol 67:390–400 (1983).
5. Lutz RJ, Dedrick RL, Tuey D, Sipes IG, Anderson MW, Matthews HB. Comparison of the pharmacokinetics of several polychlorinated biphenyls in mouse, rat, dog, and monkey by means of a physiological pharmacokinetic model. Drug Metab Dispos 12:527–535 (1984).
6. Clewell HJ III, Andersen ME. Risk assessment extrapolations and physiological modeling. Toxicol Ind Health 1:111–131 (1985).
7. Andersen ME, Clewell HJ III, Gargas ML, Smith FA, Reitz

RH. Physiologically based pharmacokinetics and the risk assessment process for methylene chloride. Toxicol Appl Pharmacol 87:185–205 (1987).
8. Ramsey JR, Andersen ME. A physiologically based description of the inhalation pharmacokinetics of styrene in rats and humans. Toxicol Appl Pharmacol 73:159–175 (1984).
9. Gargas ML, Andersen ME. Clewell HJ III. A physiologically based simulation approach for determining metabolic constants from gas uptake data. Toxicol Appl Pharmacol 86:341–352 (1986).
10. Jepson GW. A kinetic model for acetylcholinesterase inhibition by diisopropylfluorophosphate in crude rat brain homogenate. M.S. Thesis. Dayton, Ohio: Wright State University, 1986.
11. Maxwell DM, Vlahacos CP, Lenz DE. A pharmacodynamic model for soman in the rat. Toxicol Lett 43:175–188 (1988).
12. Taylor P. Anticholinesterase agents. In: The Pharmacological Basis of Therapeutics (Gilman AG, Goodman LS, Gilman A, eds). New York:Macmillan Publishing, 1980;100–1199.
13. Maxwell DM, Lenz DE, Groff WA, Kaminskis A, Froehlich HL. The effects of blood flow and detoxification on *in vivo* cholinesterase inhibition by soman in rats. Toxicol Appl Pharmacol 88:66–76 (1987).
14. Mazur A. An enzyme in animal tissue capable of hydrolyzing the phosphorous-fluorine bond of alkyl fluorophosphates. J Biol Chem 164:271–289 (1946).
15. De Bisschop HC, Van Driessche EE, Alberty MLM, Willems JL. *In vitro* detoxification of soman in human plasma. Fundam Appl Toxicol 5:S175–S179 (1985).
16. Wallace KB, Dargan JE. Intrinsic metabolic clearance of parathion and paraoxon by livers from fish and rodents. Toxicol Appl Pharmacol 90:235–242 (1987).
17. Chemnitius JM, Losch H, Losch K, Zech R. Organophosphate detoxicating hydrolyases in different vertebrate species. Comp Biochem Physiol 76C:85–93 (1983).
18. Pla A, Johnson MK. Degradation by rat tissues *in vitro* of organophosphorus esters which inhibit cholinesterase. Biochem Pharmacol 38(9):1527–1533 (1989).
19. Schaffer NK, May CS, Summerson WH. Serine phosphoric acid from diisopropylphosphoryl derivative of eel cholinesterase. J Biol Chem 206:201–207 (1954).
20. Clement JG. Role of aliesterase in organophosphate poisoning. Fundam Appl Toxicol 4:S96–S105 (1984).
21. Vandekar M, Heath DF. The reactivation of cholinesterase after inhibition *in vivo* by some dimethyl phosphate esters. Biochem J 67:202-208 (1957).
22. Behrends F, Posthumus CH, Sluys Ivd, Deierkauf FA. The chemical basis of the "aging process" of DFP-inhibited pseuodocolin-esterase. Biochim Biophys Acta 34:576–578 (1959).
23. Wenthold RJ, Mahler HR, Moore WJ. The half-life of acetylcholinesterase in mature rat brain. J Neurochem 22:941–943 (1974).
24. Michalek H, Meneguz A, Bisso GM. Mechanisms of recovery of brain acetylcholinesterase in rats during chronic intoxication by isoflurophate. Arch Toxicol (Suppl 5):116–119 (1982).
25. Traina ME, Serpietri LA. Changes in the levels and forms of rat plasma cholinesterase during chronic diisopropylphosphorofluoridate intoxication. Biochem Pharmacol 33:645–653 (1984).
26. Grubic Z, Sketelj J, Klinar B, Brzin M. Recovery of acetylcholinesterase in the diaphragm, brain, and plasma of the rat after irreversible inhibition by soman: a study of cytochemical localization and molecular forms of the enzyme in the motor end plate. J Neurochem 37:909–916 (1981).
27. Hansen D, Schaum E, Wasserman O. Serum level and excretion of diisopropylfluorophosphate (DFP) in cats. Biochem Pharmacol 17:1159–1162 (1968).
28. Lehninger A. Biochemistry. New York:Worth Publishers, 1975.
29. Ward RC, Travis CC, Hetrick DM, Andersen ME, Gargas ML. Pharmacokinetics of tetrachloroethylene. Toxicol Appl Pharmacol 93:108–117 (1988).
30. Ellman G, Courtney K, Andres V Jr. A new and rapid colorimetric determination of acetylcholinesterase activity. Biochem Pharmacol 7:88–93 (1961).
31. Sato A, Nakajima T. Partition coefficients of some aromatic hydrocarbons and ketones in water, blood and oil. Br J Ind Med 36:231–234 (1979).
32. Gargas ML, Burgess RJ, Voisard DE, Cason GH, Andersen ME. Partition coefficients of low-molecular-weight volatile chemicals in various liquids and tissues. Toxicol Appl Pharmacol 97:87–99 (1989).
33. Jepson GW, Hoover DK, Black RK, McCafferty JD, Mahle DA, Gearhart JM. Partition coefficient determination for nonvolatile and intermediate volatility chemicals in biological tissues. Toxicologist 12:262 (1992).
34. Martin BR. Biodisposition of [^{3}H]Diisopropylfluorophosphate in mice. Toxicol Appl Pharmacol 77:275–284 (1985).
35. Conolly RB, Cramer J, Andersen ME. A physiologically based model for rat hepatic glutathione (GSH): its circadian oscillation and interaction with halogenated hydrocarbons. Pharmacologist 28:211 (1986).
36. D'Souza RW, Francis WR, Andersen ME. Physiological model for tissue glutathione depletion and increased resynthesis after ethylene dichloride exposure. J Pharmacol Exp Ther 245(Suppl 2):563–568 (1988).
37. Eigenberg DA, Pazdernik TL, Doull J. Hemoperfusion and pharmacokinetic studies with parathion and paraoxon in the rat and dog. Drug Metab Dispos 11(Suppl 4):366–370 (1983).
38. Reitz RH, Mendrala AL, Guengerich FP. *In vitro* metabolism of methylene chloride in human and animal tissues: use in physiologically based pharmacokinetic models. Toxicol Appl Pharmacol 97:230–246 (1989).
39. Wilkinson GR. Prediction of *in vivo* parameters of drug metabolism and distribution from *in vitro* studies. Drinking Water and Health 8:80–95 (1987).
40. Andersen RA, Laake K, Fonnum F. Reactions between alkyl phosphates and acetylcholinesterase from different species. Comp Biochem Physiol 42B:429–437 (1972).
41. Carson VG, Jednen DJ, Russell RW. Changes in peripheral cholinergic systems following development of tolerance to the anticholinestease diisopropyl fluorophosphate. Toxicol Appl Pharmacol 26:39–48 (1973).
42. Ehlert FJ, Kokka N, Fairhurst AA. Altered [^{3}H]quinuclidinyl benzilate binding in the striatum of rats following chronic cholinesterase inhibition with diisopropylfluorophosphate. Mol Pharmacol 17:24-30 (1980).
43. Yamada S, Isogai M, Hayashi E. Correlation between cholinesterase inhibition and reduction in muscarinic receptors and choline uptake by repeated diisopropylfluorophosphate administration: antagonism by physostigmine and atropine. J Pharmacol Exp Ther 226:519–525 (1983).
44. Tsujita T, Okuda H. Carboxylesterases in rat and human sera and their relationship to serum aryl acylamidases and cholinesterases. Eur J Biochem 133:215–220 (1983).
45. Clewell HJ III, Andersen ME. Improving toxicology testing protocols using computer simulations. Toxicol Lett 49:139–158 (1989).
46. Albuquerque EX, Akaike A, Shaw AP, Rickett DL. The interaction of anticholinesterase agents with the acetylcholine receptor-ion channel complex. Fundam Appl Toxicol 4:S27–S33 (1984).
47. Grob D, Lilienthal JL Jr, Harvey AM, Jones BF. The administration of diisopropyl fluorophosphate (DFP) to man, I. Bull - Johns Hopkins Hosp 81:217–243 (1947).